Estimating Airborne Transmission Risk for Indoor Space: Coupling Agent-based Model and Computational Fluid Dynamics

Boon Leng Ang[1], Jaeyoung Kwak[1], Chin Chun Ooi[2], Zhengwei Ge[2], Hongying Li[2], Michael H. Lees[3], and Wentong Cai[1]

[1] Nanyang Technological University, Singapore 639798, Singapore
bang013@e.ntu.edu.sg, {jaeyoung.kwak, hongying.li, aswtcai}@ntu.edu.sg
[2] Institute of High Performance Computing, Singapore 138632, Singapore
{ooicc, ge_zhengwei, lih}@cfar.a-star.edu.sg
[3] University of Amsterdam, Amsterdam 1098XH, The Netherlands
m.h.lees@uva.nl

Abstract. The emergence of coronavirus disease (COVID-19) in late 2019 sparked a global pandemic, profoundly impacting societies and economies worldwide. To mitigate its spread, governments have implemented various preventive measures, prompting extensive research into transmission risk assessment. To evaluate the transmission risk systematically, we developed a framework integrating agent-based modeling (ABM) and computational fluid dynamics (CFD), and applied the framework to a preschool COVID-19 cluster in Singapore as a case study. Individual movement and behaviors are simulated with ABM, and CFD is employed to compute virus particle flow which is critical for transmission risk. In the case study, we categorized the infected individual's movement into three types based on the initial destinations and evaluated its impact on the transmission risk. Simulation results show that the average risk level is nearly the same for all three movement types and it changes across time depending on the degree of infected individual's active movement.

Keywords: Computational Fluid Dynamics (CFD) · Agent-Based Modeling (ABM) · Transmission Risk.

1 INTRODUCTION

For several decades, the study of human crowds has been crucial in real-world applications, such as planning effective evacuation [4], studying disease transmission [8], and simulating virtual crowds for computer graphics [24]. This is especially relevant to the 2019 novel coronavirus disease (COVID-19) global pandemic that began in December 2019 [15]. As of January 2024, the pandemic has led to 774 million infections and taken the lives of 7 million people, severely and permanently affecting the livelihood and work of people across the world [19].

To curb the spread of the coronavirus, many nations have taken a variety of preventive measures such as vaccination campaigns, enforcing mask-wearing,

ICCS Camera Ready Version 2025
To cite this paper please use the final published version:
DOI: 10.1007/978-3-031-97626-1_16

and practicing social distancing. Extensive research has been conducted to evaluate the effectiveness of such measures. One stream of research focuses on the movement of individuals in line with agent-based model (ABM) and evaluating the transmission risk based on the inter-personal distance [21]. A diverse range of scenarios have been studied, such as supermarkets [27], train stations [13], and university campuses [1]. This type of approach allows us to make a straightforward estimation, but air flow is not considered although it is critical for airborne disease transmissions.

Another stream of research is based on computational fluid dynamics (CFD) simulations, which aim to compute the flow of droplets and aerosols in the air and the subsequent amount inhaled by individuals [18, 20, 29]. Although this approach can reflect details of virus particle dispersion in the air, most studies assume that individuals are stationary.

A few studies have proposed integrating ABM approach with CFD simulation. For instance, Vuorinen *et al.* [28] applied Monte-Carlo modeling for simulating the movement of susceptible and infected individuals, and CFD simulations to estimate the spread of aerosols and droplets in built environment such as a library and pub. In another study, Mendez *et al.* [16] simulated droplet trajectories in line with CFD simulations, aggregated the viral concentration at individual level, and then coupled the estimated concentration with pedestrian trajectories collected from different public places like train stations, markets, and street cafés. Those studies focused on transport of aerosol and droplets, for instance, aerodynamic effects like air flow and human motion, and droplet and aerosol dispersion and their behavior in indoor airflow.

In this work, we present an extension of the integration of ABM and CFD for the estimation of airborne transmission risk for indoor space. While the previous work [16, 28] studied hypothetical scenarios, we applied our approach for various individual movement patterns for a preschool COVID-19 cluster in Singapore as a case study. Based on the available information of dimensions and air flow conditions of the study venue, we performed a series of crowd simulations to generate possible trajectories of individuals, computed location-specific virus particle concentration, and then integrated both components to systematically evaluate the airborne disease transmission risk.

The remainder of this paper is organized as follows: Section 2 gives a literature review on related work. Section 3 presents the simulation layout and the underlying models for individual movement and behaviors, and transmission risk evaluation. Section 4 presents the numerical experiments and discusses the results. We also have a discussion on the results as well as the limitations of the case study. Section 5 summarizes our work and provides possible research directions for the future.

ICCS Camera Ready Version 2025
To cite this paper please use the final published version:
DOI: 10.1007/978-3-031-97626-1_16

2 Related Work

2.1 Crowd Simulations

There are differences in granularity when it comes to choosing the appropriate crowd simulation models. A few approaches including flow-based model and agent-based model have been developed to understand and replicate crowd behaviors [22]. In the flow-based model, individuals are portrayed as part of homogeneous crowds sharing common behaviors and destinations. This model is suitable for studying aggregate behavior in large gatherings showing homogeneous behaviors, for instance, walking toward the same destination [7]. On the other hand, the agent-based model represents individuals as members of heterogeneous crowds, each possessing intellectual capacity, unique traits, and the ability to react to others and their surroundings. This model is suitable for simulating pedestrian flow in a busy facility where we can see complex crowd dynamics in terms of various walking directions and constantly changing pedestrian volumes [6].

In many human crowd studies, agent-based simulation has emerged as the dominant approach for modeling crowds due to its ability to simulate detailed and complex environments. This is achieved by representing individuals as intelligent agents, thereby allowing for a more accurate depiction of the diverse aspects of human behaviors in the real world [14]. In a scoping review by Sun *et al.* [23], agent-based model has gained popularity in studying the effectiveness of policy intervention for COVID-19.

2.2 Infection Risk Models

With regards to the research into infection risk assessment of respiratory disease transmission, two approaches have been widely applied: the Wells-Riley model and dose-response model [25]. Wells-Riley is a simpler model predicting the risk of infection based on the concentration of infectious particles in the air and the duration of exposure. On the other hand, the dose-response model examines the risk of a response such as infection and illness severity due to a quantity (dose) of infectious particles.

In line with the dose-response model, Bale *et al.* [2] applied breathing zones to quantify the amount of virus particles an individual is exposed to. A breathing zone is defined to be a region of 3D space where particles are likely to be inhaled by an agent. The shape and dimensions of this region is theoretically arbitrary, but it is typically situated in front of an agent's nose and mouth. The authors assumed breathing zone dimensions of $10 \times 10 \times 15$ cm^3 which was further divided into 16 equally sized mesh blocks. Bale *et al.* [2] applied the concept of breathing zone for the estimation of individuals' virus particle exposure level.

ICCS Camera Ready Version 2025
To cite this paper please use the final published version:
DOI: 10.1007/978-3-031-97626-1_16

3 Model

3.1 Scenario

For the case study, we modeled an outbreak at a preschool in Singapore, based on information reported by local news outlets [17, 26]. One day, a staff of the preschool center was organizing a training session along with 30 staff members from other preschool centers. A few days later, it was found that the training session organizer was infected with COVID-19 when she was leading the session. According to the local news outlets, all the training session attendees had contact with the infected person and at least 16 of them were infected.

As not many details of the outbreak are available to us, we have made several assumptions on agent behaviors to develop the scenario. We first assumed a 15-minute break in the middle of the training session. Before the break, the session organizer was standing in front of other attendees who were sitting at the table. In addition, the session organizer was leading the session and giving a presentation while other attendees were listening to her. Once the break began, all the attendees were standing and walking around the preschool center. This break time will subsequently be the focus of this study because the amount of interaction among the attendees would be significant in terms of investigating the level of virus particle exposure.

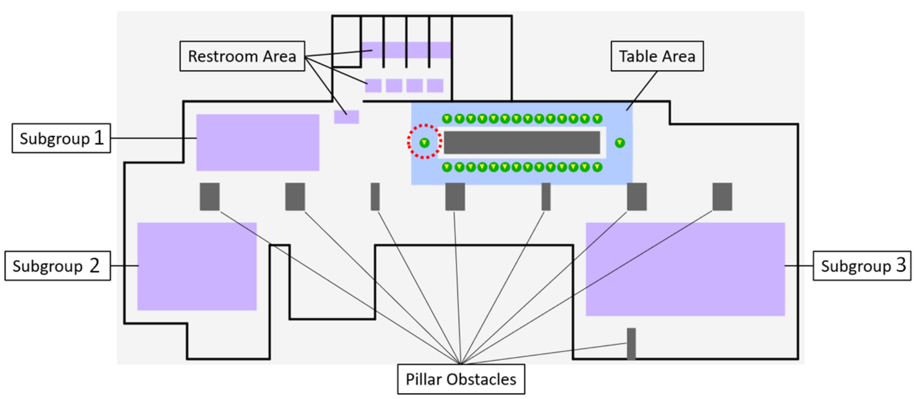

Fig. 1. The sketch of preschool scenario. The green circles represent the attendees. The contagious individual (session organizer) is indicated by a red dotted circle.

Figure 1 shows the sketch of preschool layout, which is created based on existing preschools in Singapore. As can be seen from Figure 1, the scenario can be separated into three different sections: table area, restroom area, and subgroup areas. In the table area, all 30 attendees are seated around the rectangular table during the training session. Specifically, 1 person each on the east and west

ICCS Camera Ready Version 2025
To cite this paper please use the final published version:
DOI: 10.1007/978-3-031-97626-1_16

side, 14 persons each on the north and south side. The session organizer, who is the first infected person among the attendees, is indicated by a red dotted circle in Figure 1. When the 15-minute break begins, everyone will leave their seats to visit other areas. The restroom area is a unisex facility consisting of an entrance, 4 cubicles, and 4 sinks. Before entering, people will form a queue at the restroom entrance. Upon entering, they will enter one of the 4 available cubicles with equal probability. After that, they will use the sink in front of the cubicle, before exiting the restroom. There are 3 subgroup areas in the preschool where individuals can gather and have casual conversations during the break.

3.2 Pedestrian Model

Our pedestrian movement model is implemented in MomenTUMv2 [10] based on the concept of hierarchical behavior modeling which describes the pedestrian behavior in terms of three interconnected layers: the strategic layer, the tactical layer and the operational layer [3, 5].

The strategic layer is related to the destination choice. We used origin-destination (OD) matrix, which specifies the probability of a pedestrian visiting one area from another area. When the break begins, the attendees can either use the restroom, join a subgroup, or stay at their table seats. Additionally, the attendees that have used the washroom will either return to the table or join a subgroup. Over time, individuals will gradually leave the subgroups and return to the table. Figure 2 summarizes the movement flow of the pedestrians with a flowchart and Figure 3 shows all the possible routes.

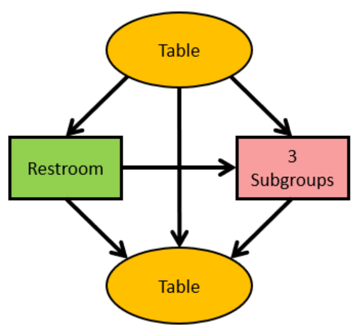

Fig. 2. Flowchart of attendee movement during the break

The tactical layer is about how pedestrians approach their destinations. As the venue size of the preschool is small, we assume that the pedestrians have complete knowledge of all destinations. Hence, we utilized models that are computationally less intensive: Djikstra's algorithm to find the shortest route to the destinations and shifted random participating model to simulate pedestrian behavior of finding a position in a subgroup [11].

ICCS Camera Ready Version 2025
To cite this paper please use the final published version:
DOI: 10.1007/978-3-031-97626-1_16

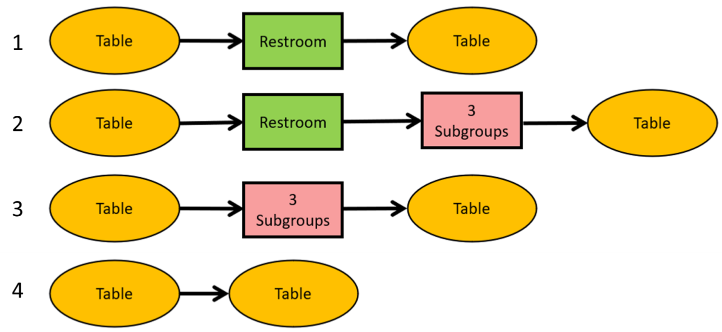

Fig. 3. All possible routes that an attendee can take

The operational layer is associated with step-by-step movements during walking, queuing, and standing. We applied the social force model to simulate the walking behavior of pedestrians. As for the standing behavior, we utilized the model developed by Johansson *et al.* [9], so that we can ensure that the pedestrians in a queue stay responsive between standing and moving along the washroom queue. For the standing behavior, we implemented the Fixed standing model which prevents pedestrians in a subgroup from shuffling excessively when they are conversing at the spacious areas [12].

3.3 Exposure Level Estimation Model

We first computed the location-specific concentration of virus particles emitted by the contagious individual by means of computational fluid dynamics (CFD) simulations. Based on the work of Ooi *et al.* [18], we numerically solved the Navier-Stokes equation for conservation of mass and momentum, and the energy equation using a computational fluid dynamics (CFD) software (ANSYS FLUENT version 21.2). For simplicity, we assumed that the virus particle concentration level is in steady-state during the break in that the virus particles concentration level increased during the training session before the break. The virus particles concentration level does not change in the course of time during the break, thus we mainly consider the position of the contagious individual and other (i.e., susceptible) attendees, and the virus particle concentration around the susceptible individuals reflects the amount of inhaled virus particles. The mesh resolution of CFD simulations is around 10 cm.

Based on the study of Bale *et al.* [2], we assumed a $50 \times 50 \times 50$ cm^3 cubic region as the breathing zone. For the preschool scenario, the breathing zone was further simplified to be 50×50 cm^2 rectangular area from a top-down 2D view. This simplification was done because it was assumed that all attendees were roughly the same height and standing during the 15-minute break, and hence their breathing zones would be located on the same 2D plane. The breathing zone was divided into a 10×10 cm^2 grid in line with the spatial resolution of virus particle concentration estimation. The coordinates of the 25 grid square centers

ICCS Camera Ready Version 2025
To cite this paper please use the final published version:
DOI: 10.1007/978-3-031-97626-1_16

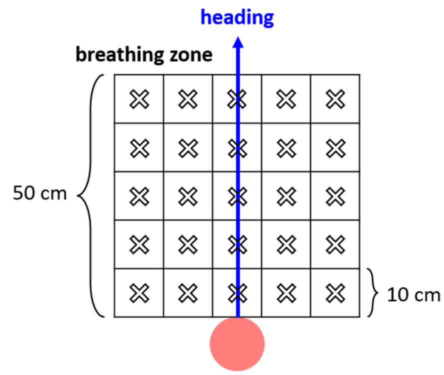

Fig. 4. 2D view of an attendee's breathing zone (not drawn to scale). A breathing zone contains 25 grid squares and the cross ($\times$) symbols indicate the center of grid squares. The breathing zone is attached to an attendee which is represented as a red circle.

were used to calculate the representative value of virus particle concentration for a breathing zone. Additionally, the breathing zone is located in front of an agent, where the midpoint of the breathing zone bottom side touches the attendee's boundary. Figure 4 illustrates the setup of an attendee's breathing zone.

Using the pedestrian trajectory generated by MomenTUMv2 software, for each time frame, we obtained the coordinates of the contagious and susceptible individuals, and the headings of the susceptible individuals along with the coordinates of the 25 grid points in their breathing zone (50×50 cm^2 rectangular area in Figure 4). For each susceptible individual, we computed the representative particle concentration value of the breathing zone by taking average of virus particle concentration at each grid point within the breathing zone. We then estimated the exposure level for each individual by summing the representative value of virus particle concentration for all time frames. It is noted that we computed the virus particle concentration as a proxy for an attendee's level of exposure to virus particles. This measure is related to the infection risk in that the larger the concentration, the higher the virus particle exposure level and infection risk.

The code that we used in this paper are available on github: `https://github.com/jaeyoung82/iccs2025-ABM-CFD`.

4 Simulation Results

In this section, we utilize the presented framework to perform a series of numerical experiments to evaluate how the initial destination of the sole contagious individual can affect the virus particle exposure level of other individuals in the scenario. In doing that, we performed three numerical experiments:

- Experiment R: The contagious individual goes to the restroom (R) first once the break starts, optionally joins a subgroup to talk with others, and then

ICCS Camera Ready Version 2025
To cite this paper please use the final published version:
DOI: 10.1007/978-3-031-97626-1_16

goes back to the table before the break ends. Refer to routes 1 and 2 shown in Figure 3.

– Experiment G: The contagious individual joins one of three subgroups (G) to talk with others once the break starts, and then goes back to the table before the break ends. Refer to route 3 shown in Figure 3.
– Experiment T: The contagious individual stays at the table (T) during the break, not walking around in the room. Refer to route 4 shown in Figure 3.

For each experiment, we randomly assigned six individuals for each initial destination: restroom, subgroups 1, 2, 3, and table. We conducted 30 runs for each experiment (R, G, T) with random initial destinations of the susceptible individuals. For experiment G, we performed 10 runs for each subgroup (subgroups 1, 2, and 3). It is noted that three most probable initial destinations of the infected individual were selected as her actual movement trajectory is unknown.

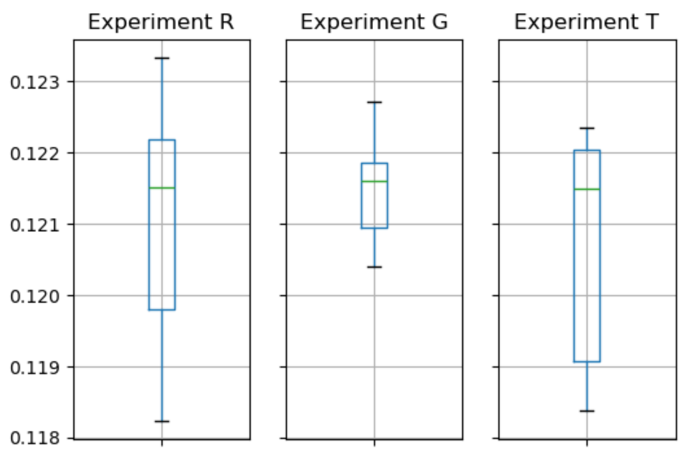

Fig. 5. Boxplots of individual's virus particle exposure level for each experiment. Note that the y-axis does not start at zero, focusing on the effective range between the minimum and maximum values.

Figure 5 shows boxplots of individual's virus particle exposure level for each experiment, reflecting the distribution of estimated transmission level. The average value of the individual's exposure level is nearly the same for all three experiments. This appears to be because the virus particle concentration level is assumed to be in steady-state. In addition, it can be seen that experiments R and T yield considerable variation, but the variation is less notable for experiment G. One can also notice that the level of virus particle exposure is positive for every susceptible individual regardless of the experiment type. This is because the virus particles were spreading in the scenario during the training session before the break, so the virus particle concentration level is considerable everywhere in the scenario.

ICCS Camera Ready Version 2025
To cite this paper please use the final published version:
DOI: 10.1007/978-3-031-97626-1_16

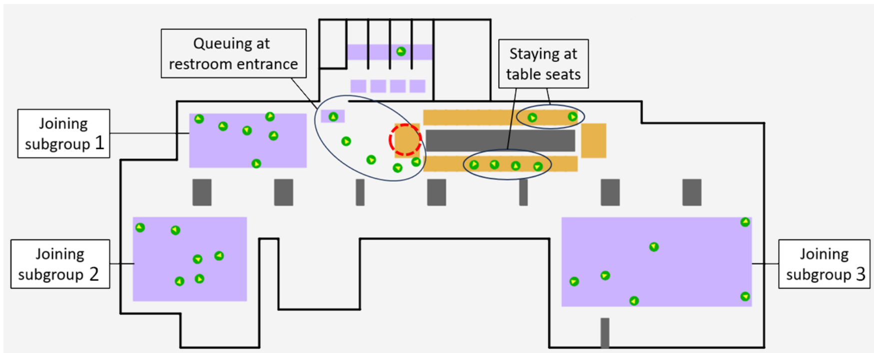

Fig. 6. A sample screenshot showing spatial distribution of training session attendees. The red dotted circle indicates the position of the contagious individual where she would stay in experiment T.

This can be understood in terms of how much the contagious individual moves actively. In experiment R, it is possible for the contagious individual to walk the longest route by possibly visiting both the restroom and subgroup areas. In addition, attendees queuing at the restroom can encounter the contagious individual when she enters and leaves the restroom. For experiment T, the contagious individual stays at the table, but attendees in subgroups 1 and 2 need to bypass her and attendees queuing at the restroom might be exposed to her, see an example from Figure 6. In contrast, for experiment G, the contagious individual goes to a subgroup almost immediately and tends to meets less individuals compared to other experiments.

The impact of distance between the contagious and susceptible individuals on the virus particle exposure level can be inferred from Spearman's correlation coefficient. As can be seen from Table 1, experiment T has strong correlation and experiment R has moderate correlation, while experiment G shows weak correlation between the two variables. It can be suggested that only considering the distance between contagious and susceptible individuals might not be enough to estimate the transmission risk, thus the inclusion of CFD is substantial in the risk estimation. In addition, for experiment G, susceptible individuals' virus particle exposure level is seemingly attributed to the virus particles in the air rather than the one emitted from the infected individual, thus the variation of virus particle exposure level is less significant among the susceptible individuals.

Furthermore, we plotted time series graphs to examine how the transmission risk changes in the course of time, see Figure 7. It can be observed that all three graphs dip down to varying degree at start of the break, remain stable from minutes 3 to 10, and then quickly increase between minutes 12 and 14. It appears that the appearance of the plateau is attributed to the spatial distribution of attendees in that the attendees do not actively walk around the preschool center. The rapid increase from minutes 12 to 14 is seemingly due to the attendees' be-

ICCS Camera Ready Version 2025
To cite this paper please use the final published version:
DOI: 10.1007/978-3-031-97626-1_16

Table 1. Correlation between the estimated transmission risk level and the distance between infected and susceptible individuals

Experiment	Correlation
R	-0.5414
G	0.0269
T	-0.9181

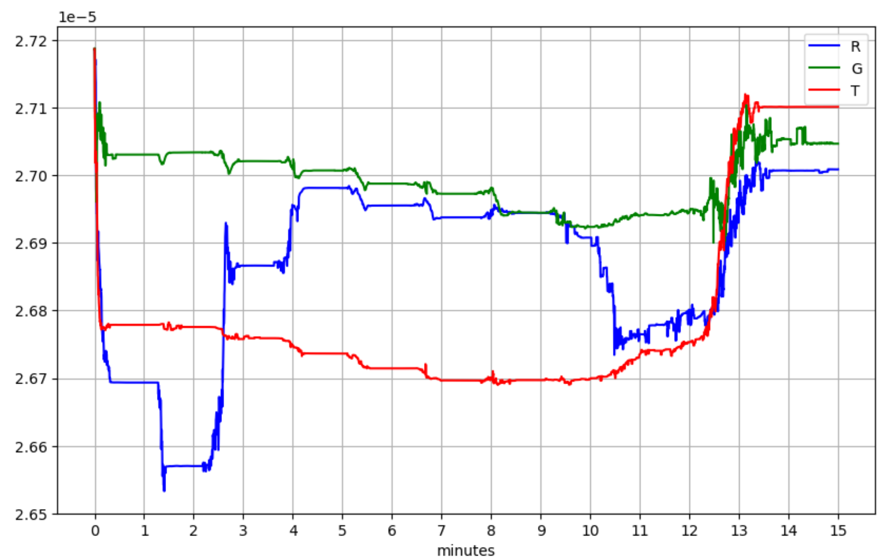

Fig. 7. Time series of transmission risk estimated for all three experiments. Note that the y-axis does not start at zero, zooming in the range of interest.

havior of returning to the table. In addition, the curve of experiment R increases sharply between minutes 2 and 3. It is likely that the the queuing attendees encounter the contagious individual when she leaves the restroom while walking to the table or a subgroup.

5 Conclusion

We present a framework integrating agent-based modeling (ABM) and computational fluid dynamics (CFD) to systematically evaluate the airborne disease transmission risk. We modeled the movement of individuals in line with ABM and estimated virus particle concentration level based on CFD simulations. As a case study, the framework was applied to a preschool COVID-19 cluster in Singapore. We categorized the infected individual's movement into three types based on the initial destination and evaluated its impact on the transmission

ICCS Camera Ready Version 2025
To cite this paper please use the final published version:
DOI: 10.1007/978-3-031-97626-1_16

risk level. Simulation results show that the average risk level is nearly the same for all three movement types but it changes across time depending on the degree of infected individual's active movement.

Our study demonstrated potential in coupling ABM and CFD to estimate the airborne disease transmission risk, and the presented framework can be applied to different scenarios where the air flow condition is critical for the disease transmission risk. Although the presented results are produced based on a simple scenario, our study demonstrated potential in coupling ABM and CFD to estimate the airborne disease transmission risk for a real-world case in Singapore. The results are still useful for evaluating the airborne disease transmission risk and comparing possible movement of the contagious person in the scenario.

A limitation of the study is that we did not explicitly consider various respiratory activities (such as speaking, coughing, and singing) for simplicity. Computation of the aerosol and droplet dispersion reflecting such respiratory activities will allow us to better study the transmission risk as respiratory activities are highly relevant to the infectiousness and rapid spread of airborne diseases [2]. While this study used a 2D CFD model with point-to-point movement trajectories of individuals to make transmission risk evaluation simple, a 3D CFD model would provide greater model fidelity. In addition, a few simple experiments were designed and tested due to the lack of detailed information for the outbreak. The presented ABM can be further improved with more information of the attendees' behavior, for instance, their activity patterns before and after the training session, and during the whole session. Furthermore, the presented framework can be extended to estimate the critical amount of virus particle exposure level if it is known which attendees were infected. Another possible future work is to examine the impact of non-pharmaceutical control measures, for instance, social distancing, ventilation, and wearing a mask.

Acknowledgments. This research is supported by the Singapore Ministry of Health's National Medical Research Council under its National Epidemic Preparedness and Response R&D Funding Initiative (MOH-001041) Programme for Research in Epidemic Preparedness And REsponse (PREPARE).

Disclosure of Interests. The authors have no competing interests to declare that are relevant to the content of this article.

DOI: 10.1007/978-3-031-97626-1_16

References

1. Alvarez Castro, D., Ford, A.: 3d agent-based model of pedestrian movements for simulating covid-19 transmission in university students. ISPRS International Journal of Geo-Information **10**, 509 (2021)
2. Bale, R., Iida, A., Yamakawa, M., Li, C., Tsubokura, M.: Quantifying the covid19 infection risk due to droplet/aerosol inhalation. Scientific Reports **12**, 11186 (2022)
3. Daamen, W.: Modelling passenger flows in public transport facilities. Phd dissertation, Delft University of Technology, Delft, the Netherlands (2004), `https://repository.tudelft.nl/islandora/object/uuid:e65fb66c-1e55-4e63-8c49-5199d40f60e1`, accessed April 11th, 2024
4. Helbing, D., Farkas, I., Vicsek, T.: Simulating dynamical features of escape panic. Nature **407**, 487–490 (2000)
5. Hoogendoorn, S., Bovy, P.: Pedestrian route-choice and activity scheduling theory and models. Transportation Research Part B: Methodological **38**, 169–190 (2004)
6. Hoy, G., Morrow, E., Shalaby, A.: Use of agent-based crowd simulation to investigate the performance of large-scale intermodal facilities: case study of union station in toronto, ontario, canada. Transportation Research Record **2540**, 20–29 (2016)
7. Hughes, R.: A continuum theory for the flow of pedestrians. Transportation Research Part B: Methodological **10**, 2205255 (2002)
8. Johansson, A., Batty, M., Hayashi, K., Al Bar, O., Marcozzi, D., Memish, Z.: Crowd and environmental management during mass gatherings. The Lancet Infectious Diseases **12**, 150–156 (2012)
9. Johansson, F., Peterson, A., Tapani, A.: Waiting pedestrians in the social force model. Physica A: Statistical Mechanics and its Applications **419**, 95–107 (2015)
10. Kielar, P., Biedermann, D., Borrmann, A.: Momentumv2: A modular, extensible, and generic agent-based pedestrian behavior simulation framework. Tech. rep., Technische Universität München, Munich, Germany (2016)
11. Kielar, P., Borrmann, A.: Coupling spatial task solving models to simulate complex pedestrian behaviour patterns. In: In Proceedings of the 8th Conference on Pedestrian and Evacuation Dynamics. pp. 229–235 (2016)
12. Kielar, P., Borrmann, A.: Modeling pedestrians' interest in locations: A concept to improve simulations of pedestrian destination choice. Simulation Modelling Practice and Theory **61**, 47–62 (2016)
13. Lee, J., Marinov, M.: Analysis of rail passenger flow in a rail station concourse prior to and during the covid-19 pandemic using event-based simulation models and scenarios. Urban Rail Transit **8**, 99–120 (2022)
14. Luo, L., Chai, C., Ma, J., Zhou, S., Cai, W.: Proactivecrowd: Modelling proactive steering behaviours for agent-based crowd simulation. Computer Graphics Forum **37**, 375–388 (2018)
15. Maxmen, A.: Who report into covid pandemic origins zeroes in on animal markets, not labs. Nature **592**, 173––174 (2021)
16. Mendez, S., Garcia, W., Nicolas, A.: From microscopic droplets to macroscopic crowds: Crossing the scales in models of short-range respiratory disease transmission, with application to covid-19. Advanced Science **10**, 2205255 (2023)
17. Mothership: Covid-19: Sparkletots preschool cluster increases to 20 cases, forming 3rd largest local cluster (2020), accessed: April 22nd, 2025, `https://mothership.sg/2020/03/covid-19-sparkletots-preschool-coi/`
18. Ooi, C., Suwardi, A., Ou Yang, Z., Xu, G., Tan, C., Daniel, D., Li, H., Ge, Z., Leong, F., Marimuthu, K., Ng, O.: Risk assessment of airborne covid-19 exposure in social settings. Physics of Fluids **33**, 087118 (2021)

ICCS Camera Ready Version 2025
To cite this paper please use the final published version:
DOI: 10.1007/978-3-031-97626-1_16

19. Our World in Data: Coronavirus pandemic (covid-19) (2020), published online at OurWorldInData.org. Retrieved from https://ourworldindata.org/coronavirus
20. Peng, S., Chen, Q., Liu, E.: The role of computational fluid dynamics tools on investigation of pathogen transmission: Prevention and control. Science of The Total Environment **746**, 142090 (2021)
21. Ronchi, E., Lovreglio, R.: Exposed: An occupant exposure model for confined spaces to retrofit crowd models during a pandemic. Safety Science **130**, 104834 (2020)
22. Saeed, R., Recupero, D., Remagnino, P.: Modelling group dynamics for crowd simulations. Personal and Ubiquitous Computing **26**, 1299–1319 (2022)
23. Sun, Z., Bai, R., Bai, Z.: The application of simulation methods during the covid-19 pandemic: A scoping review. Journal of Biomedical Informatics **148**, 104543 (2023)
24. Sung, M., Gleicher, M., Chenney, S.: Scalable behaviors for crowd simulation. Computer Graphics Forum **23**, 519–528 (2004)
25. Sze To, G., Chao, C.: Review and comparison between the wells–riley and dose-response approaches to risk assessment of infectious respiratory diseases. Indoor Air **20**, 2–16 (2010)
26. Today Online: 49-year-old preschool staff among 373 new covid-19 cases (2020), accessed: April 22nd, 2025, https://www.todayonline.com/singapore/new-covid-19-cases-may-28
27. Tsukanov, A., Senjkevich, A., Fedorov, M., Brilliantov, N.: How risky is it to visit a supermarket during the pandemic? PLOS One **16**, e0253835 (2021)
28. Vuorinen, V., Aarnio, M., Alava, M., Alopaeus, V., Atanasova, N., Auvinen, M., Balasubramanian, N., Bordbar, H., Erästö, P., Grande, R., Hayward, N.: Modelling aerosol transport and virus exposure with numerical simulations in relation to sars-cov-2 transmission by inhalation indoors. Safety Science **1303**, 104866 (2020)
29. Zhang, Z., Han, T., Yoo, K., Capecelatro, J., Boehman, A., Maki, K.: Disease transmission through expiratory aerosols on an urban bus. Physics of Fluids **33**, 015116 (2021)

ICCS Camera Ready Version 2025
To cite this paper please use the final published version:
DOI: 10.1007/978-3-031-97626-1_16